7

The Measurement of Uranium Enrichment

Hastings A. Smith, Jr.

7.1 INTRODUCTION

Uranium and plutonium samples are present in the nuclear fuel cycle in a wide variety of isotopic compositions; so the isotopic composition of a sample is often the object of measurement (see Chapter 8). In this chapter, we consider a special case of isotopic analysis: the determination, by radiation measurement, of the fractional abundance of a specific isotope of an element. This measurement is most often applied to uranium samples to establish the fraction of fissile ^{235}U, commonly referred to as the *uranium enrichment*. The term "enrichment" is used because the fraction of the sample that is ^{235}U is usually higher than that in naturally occurring uranium.

Three isotopes of uranium are prevalent in nature (their isotopic atom abundances are shown in parentheses): ^{238}U (99.27%), ^{235}U (0.720%), and ^{234}U (0.006%). The ^{234}U comes from the alpha decay of ^{238}U:

$$^{238}U \xrightarrow{\alpha} {}^{234}Th \xrightarrow{\beta(24\ D)} {}^{234m}Pa \xrightarrow{\beta(1.2\ m)} {}^{234}U\ . \tag{7-1}$$

Other isotopes may be present if the sample is reactor-produced; the isotopes include ^{236}U (from neutron capture on ^{235}U) and ^{237}U [from (n,2n) reactions on ^{238}U].

The ^{235}U *atom* fraction for uranium is defined as follows:

$$E_a(\text{at\%}) = \frac{\text{No. of atoms } ^{235}U}{\text{No. of atoms U}} \times 100\ . \tag{7-2}$$

The enrichment can also be expressed as a *weight* fraction:

$$E_w(\text{wt\%}) = \frac{\text{No. of grams } ^{235}U}{\text{No. of grams U}} \times 100\ . \tag{7-3}$$

The two enrichment fractions are related by

$$E_w(\text{at\%}) = \frac{235E_a}{238\ -\ 0.03E_a} \approx \frac{235}{238}E_a\ . \tag{7-4}$$

Uranium enrichments in light-water-reactor (LWR) fuel are typically in the few percent range. CANDU reactors use natural uranium, and materials testing reactors (MTR) use highly enriched uranium (enrichments from 20% to 90%). Determination of uranium enrichment in samples is a key measurement for process or product control in enrichment and fuel fabrication plants, and is very important in international safeguards inspections to verify that uranium stock is being used for peaceful purposes.

Enrichment measurement principles can be used to determine any isotopic fraction if a radiation signature is available and if a few specific measurement conditions are met. The discussion that follows describes various enrichment measurement techniques and their applications.

7.2 RADIATIONS FROM URANIUM SAMPLES

The isotopes of uranium emit alpha, beta, neutron, and gamma radiation. The primary radiation used in passive NDA of uranium samples is gamma radiation, which is usually dominated by emissions from ^{235}U decay. However, in low-enriched uranium samples, the x radiation is the most intense component of the emission spectrum. The 185.7-keV gamma ray is the most frequently used signature to measure ^{235}U enrichment. It is the most prominent single gamma ray from any uranium sample enriched above natural ^{235}U levels. There are no common interferences except in reprocessed fuel where the 236-keV gamma ray from the ^{232}Th daughter, ^{212}Pb, usually swamps the ^{235}U line. Table 7-1 lists the most intense gamma rays from uranium isotopes of interest (see Ref. 1). Data on the alpha and neutron radiations from uranium isotopes can also be found in Ref. 1. Gamma-ray spectra from uranium samples of varying degrees of enrichment are shown in Figures 7.1 (Ref. 1) and 7.2 (Ref. 2) for high- and low-resolution gamma detectors, respectively.

7.3 INFINITE-SAMPLE GAMMA MEASUREMENT TECHNIQUE

The principles of gamma-ray uranium enrichment measurement (Refs. 3 through 5) were first applied to the measurement of UF_6 cylinders (Ref. 6). The basic measurement procedure involves viewing a uranium sample through a collimated channel with a gamma-ray detector (Figure 7.3). The enrichment is deduced from the intensity of the ^{235}U 186-keV gamma ray. If the uranium sample is large enough, the 186-keV gamma rays from only a fraction of the total sample reach the detector because of the strong absorption of typical uranium-bearing materials at this energy. This "visible volume" of the sample is determined by the collimator, the detector geometry, and the mean free path of the 186-keV radiation in the sample material. Its

size (illustrated in Figure 7.3 by the dashed lines) is independent of the enrichment because the different uranium isotopes all have the same attenuation properties. If the depth of the sample along the collimation axis is much larger than the mean free path of 186-keV photons in the sample material, all samples of the same physical composition would present the same visible volume to the detector. This is the so-called "infinite-thickness" criterion. Table 7-2 lists the mean-free-path and infinite-thickness values for the 186-keV gamma ray in commonly encountered uranium compounds. For many common uranium materials, the infinite-thickness criterion is satisfied with quite modest sample sizes. However, because we see no deeper into the sample than certain distances, as indicated in Table 7-2, gamma-ray-based enrichment measurements often sample only the *surface* of the uranium material. Then, for enrichment measurements to be meaningful for the entire sample, the material must be isotopically uniform.

Table 7-1. Gamma radiation from uranium isotopes[a]

Isotope	Gamma-Ray Energy (keV)	Specific Intensity (gamma/s-g of isotope)
^{232}U	129.1	6.5×10^8
	270.5	3.0×10^7
	327.8	2.7×10^7
^{233}U	119.0	3.9×10^4
	120.8	3.2×10^4
	146.4	6.6×10^4
	164.6	6.4×10^4
	245.3	3.8×10^4
	291.3	5.8×10^4
	317.2	8.3×10^4
^{234}U	120.9	5.4×10^5
^{235}U	143.8	7.8×10^3
	163.4	3.7×10^3
	185.7	4.3×10^4
	202.1	8.0×10^2
	205.3	4.0×10^3
^{238}U	742.8	7.1
In equilibrium	766.4	2.6×10^1
with ^{234m}Pa	786.3	4.3
	1001.0	7.5×10^1

[a]Ref. 1.

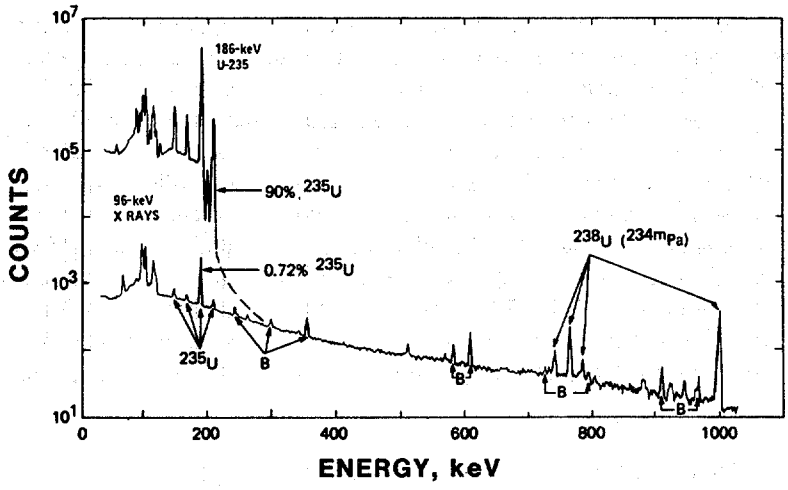

Fig. 7.1 Gamma-ray spectra from natural (0.7% ^{235}U) and 90%-enriched uranium, measured with an unshielded 14%-efficiency Ge(Li) detector. The peaks labeled ^{238}U (^{234m}Pa) are from the decay of ^{234m}Pa. Background peaks are labeled B. Note the dominance in the spectrum of the 186-keV peak from ^{235}U decay. (Figure from Ref. 1.)

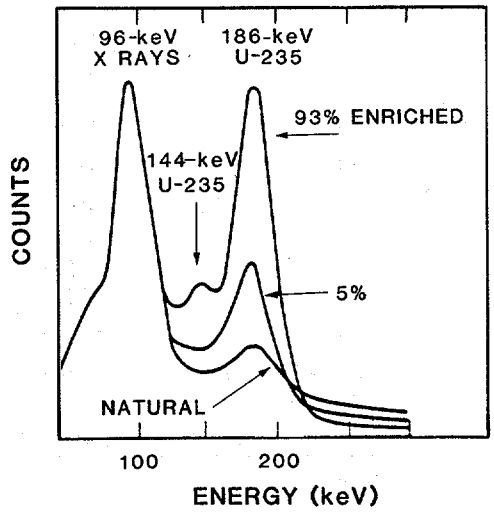

Fig. 7.2 Gamma-ray spectra from natural, 5%-enriched, and 93%-enriched uranium samples, measured with a NaI(Tl) scintillation detector. As the ^{235}U enrichment increases, the 186-keV peak becomes more intense and the background (from the ^{238}U daughters) above the peak energy becomes weaker. (Figure from Ref. 2.)

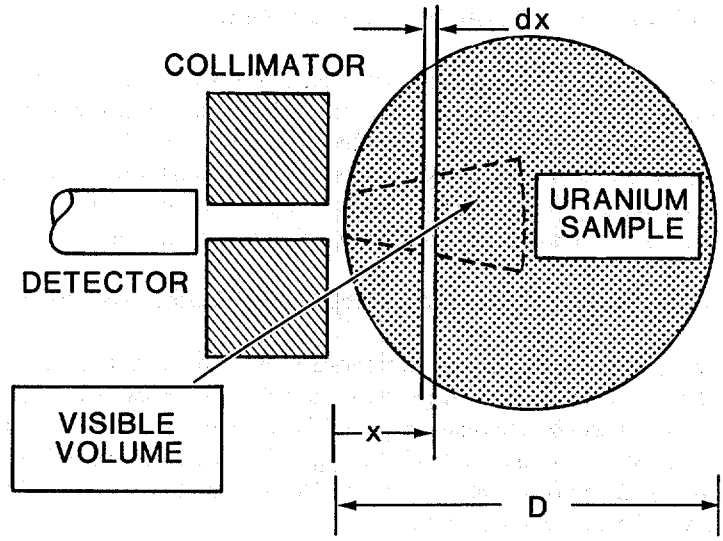

Fig. 7.3 *The basic elements of a gamma-ray uranium-enrichment measurement setup. For purposes of illustration, the size of the visible volume compared with the detector and collimator is exaggerated. Normally the depth of the visible volume is much smaller than the source-to-detector distance.*

Table 7-2. Mean free paths and infinite thicknesses for 186-keV photons in uranium compounds

Uranium Compound	Density (ρ) (g/cm^3)	Mean Free Path (cm)[a]	"Infinite" Thickness (cm)[b]
Metal	18.7	0.04	0.26
UF_6 (solid)	4.7	0.20	1.43
UO_2 (sintered)	10.9	0.07	0.49
UO_2 (powder)	2.0	0.39	2.75
U_3O_8 (powder)	7.3[c]	0.11	0.74
Uranyl nitrate	2.8	0.43	3.04

[a]Equal to $1/\mu\rho$ at 186 keV for the material in question.
[b]Defined as 7 mean free paths, the distance for which the error in assuming infinite-sample size is less than 0.1% (see Equation 7-8).
[c]Highly packed powder.

7.3.1 One-Component Example (Uranium Metal)

For a given detector/collimator geometry, all samples of pure uranium metal have identical visible volumes, since the mean free path of the 186-keV gamma ray is the same for each sample. As a result, the detector views ^{235}U radiation from the same amount of total uranium, regardless of the size of the metal sample. Since the 186-keV intensity, although heavily absorbed, is still proportional to the number of ^{235}U atoms in the visible volume, it is proportional to the *atom* enrichment of the sample.

7.3.2 Two-Component Example (Uranium and Matrix Material)

The prototypical enrichment sample consists of uranium and a (usually low-Z) matrix material. The measurement geometry is still the same as that shown in Figure 7.3, but the absorption by the matrix material is an added factor in the measurement. Exhaustive summaries of the theory of this type of measurement have been published (Refs. 7 and 8). Given below is a summary of the key mathematical results necessary to analyze enrichment measurements.

Consider a gamma-ray measurement on a two-component sample of thickness D, where the sample-to-detector distance is large compared with the depth of the visible volume. This feature permits the neglect of $1/r^2$ effects during integration over the sample volume. The counting rate from an infinitesimal section of the sample (see Figure 7.3) is given by

$$dR = \varepsilon E_w S\, dm_U \exp(-\mu\rho x) \exp(-\mu_c \rho_c t_c) \tag{7-5}$$

where $dm_U = A\ \rho_U\ dx$,

ε = detection efficiency at the assay energy

E_w = uranium enrichment (*weight* percent, see Equation 7-3)

A = collimator channel area

S = specific activity of the gamma ray (185.7 keV, see Table 7-1)

$\mu_c\rho_c$ = linear photon absorption coefficient of the sample container at the assay energy

t_c = single wall thickness of the sample container.

The quantity $\mu\rho$ represents the linear photon absorption coefficient of the combined uranium (U) and the matrix (m) at the assay energy:

$$\mu\rho = \mu_U \rho_U + \mu_m \rho_m\ . \tag{7-6}$$

Integration of Equation 7-5 over the sample thickness gives the total 186-keV count rate:

$$R = \varepsilon E_w SA\ \rho_U \exp(-\mu_c \rho_c t_c) \int_0^D \exp(-\mu\rho x)\ dx \tag{7-7}$$

which reduces to

$$E_w = \left[\frac{\mu_U}{\varepsilon SA}\right] R \left[\frac{F \exp(\mu_c \rho_c t_c)}{1 - \exp(-\mu\rho D)}\right] \tag{7-8}$$

where

$$F = 1 + (\mu_m \rho_m / \mu_U \rho_U) \, . \tag{7-9}$$

If the sample thickness D is large enough, then the exponential in the denominator of Equation 7-8 is negligible compared to 1, making variations in sample dimensions unimportant. This is the origin of the infinite-thickness criterion. The first bracket in Equation 7-8 contains factors that depend only on the instrument properties (ε and A) and the intrinsic properties of uranium (μ_U and S) and thus constitutes the basic calibration constant of the measurement. If the unknown samples and calibration standards have identical containers, then the factor, $\exp(\mu_c \rho_c t_c)$, can be subsumed into the calibration constant; otherwise the factor must be used to obtain a container correction. (See Section 7.7.)

The factor F in Equation 7-8 reflects the matrix effects. If the calibration standards and the unknown samples have the same matrix properties, then this factor can also be included in the calibration constant. If the sample matrix factor F differs from the calibration matrix factor F_s, then a small correction is also necessary for this difference. Table 7-3 gives values for this multiplicative correction (F/F_s) for various uranium compounds (Ref. 2).

Table 7-3. Material composition correction factors (F/F_s)[a]

Nuclear Material of Calibration Standards (Factor F_s)	Nuclear Material of Items Measured (Factor F)					
	U	UC	UC_2	UO_2	U_3O_8	UF_6
U (100% U)	1.00	1.00	1.00	1.01	1.01	1.04
UC (95% U)	1.00	1.00	1.00	1.01	1.01	1.03
UC_2 (91% U)	0.99	1.00	1.00	1.00	1.01	1.03
UO_2 (88% U)	0.99	0.99	1.00	1.00	1.00	1.03
U_3O_8 (85% U)	0.99	0.99	0.99	1.00	1.00	1.02
UF_6 (68% U)	0.96	0.97	0.97	0.98	0.98	1.00
U nitrate (47% U)	0.92	0.92	0.93	0.93	0.93	0.95

[a]Ref. 2.

7.3.3 Instrumentation and Infinite-Sample Technique: Applications

The basic measurement apparatus is a collimated gamma-ray detector and its associated electronics. An early version of such instrumentation was the SAM-II and a NaI(Tl) scintillation detector (Ref. 6). Gamma-ray pulses were analyzed with a dual single-channel analyzer (SCA), with one window set on the 186-keV energy region (C1 in Figure 7.4) and the second window set on a background region above the assay peak (C2 in Figure 7.4).

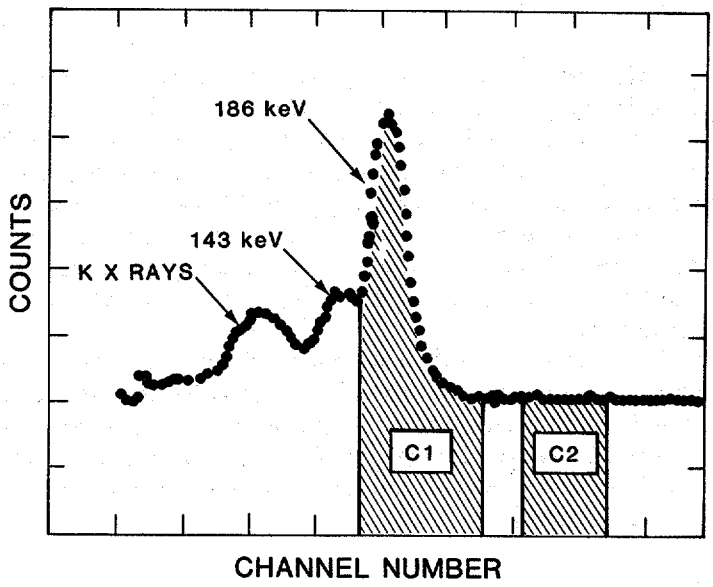

Fig. 7.4 A low-resolution uranium gamma-ray spectrum, showing the two energy regions used in the enrichment measurement.

The uranium enrichment is proportional to the *net* 186-keV count rate (R in Equation 7-8), which is given by

$$R = C1 - f\,C2\ . \qquad (7\text{-}10)$$

This equation represents the subtraction of a background from the gross rate in the chosen 186-keV peak energy region. The major contribution to the background comes from the higher energy gamma rays of ^{238}U daughters that Compton scatter in the detector. Even though C2 is not actually in the assay energy region, it represents the background under the assay region, to within a scale factor (f, to be determined by calibration). Since the enrichment (either atom or weight) is proportional to the net rate R, we have

$$E = a\ R\ F \exp(\mu_c \rho_c t_c) = F \exp(\mu_c \rho_c t_c)(a\ C1 - a\ f\ C2)\ . \quad (7\text{-}11)$$

The calibration constant a contains all of the geometric factors and the intrinsic uranium constants in Equation 7-8. The matrix factor F and the container wall attenuation correction factor $\exp(\mu_c \rho_c t_c)$ have been displayed explicitly to emphasize their roles when standards and unknowns are made of different types of materials or packaged in different containers. If the measurement is performed on materials of the same type packaged in the same container, then $F \exp(\mu_c \rho_c t_c)$ can be included in the calibration constant. The enrichment is then written in terms of the measured data (C1 and C2):

$$E = a\ C1 + b\ C2\ . \quad (7\text{-}12)$$

The calibration constants a and b (= −a f) now include the container attenuation and the matrix factor and are determined by measurement of two standards of known enrichments E_1 and E_2.

With the SAM-II, the calibration constants were applied through digital rate multipliers to the outputs of the two SCAs. An up/down scaler displayed the difference between the scaled C1 and C2 values, thereby displaying the uranium enrichment. An in-line extension of the SAM-II type of measurement has been installed at the Portsmouth Gaseous Diffusion Plant (GDP) (Ref. 9). It has been in operation for more than 12 years and continues to assay the output liquid UF_6 product with a relative accuracy of 0.25% (1σ). The instrument was developed for continuous determination of both the ^{235}U enrichment (by gamma-ray measurement) and the ^{234}U enrichment (by neutron measurement; see Section 7.6 and Chapter 15). A drawing of the gamma-ray portion of the measurement apparatus is shown in Figure 7.5.

More recent instrumentation (Ref. 10) employs a portable, battery-powered, microprocessor-based MCA with the NaI detector (Figure 7.6). The instrument acquires a full uranium spectrum, integrates the counts in selected regions of interest corresponding to the count windows C1 and C2 (for example, as in Figure 7.4), computes the enrichment and its statistical uncertainty, and presents the results on an alphanumeric display. The two-parameter, two-standard calibration procedure is also incorporated into the instrument software. A similar method is used for routine enrichment checks by some plant operators (Ref. 11). These gamma-spectroscopic techniques are used in many in-plant and field applications, including the measurement of UF_6 in storage cylinders. As with earlier measurements, many current applications still use NaI scintillation detectors (Ref. 6). However, high-resolution spectrometry with semiconductor detectors is more effective in avoiding problems of interference from ^{238}U daughters deposited on the inner surfaces of the containers. The high-resolution detector is especially helpful where chemical processes have concentrated ^{238}U daughters in the deposit or in the uranium material itself. Some commercial processes have been observed to produce up to a ten-fold concentration of ^{238}U daughters. The radiation from the daughters produces a high Compton background in the detector, which can complicate the evaluation of the 185.7-keV peak area.

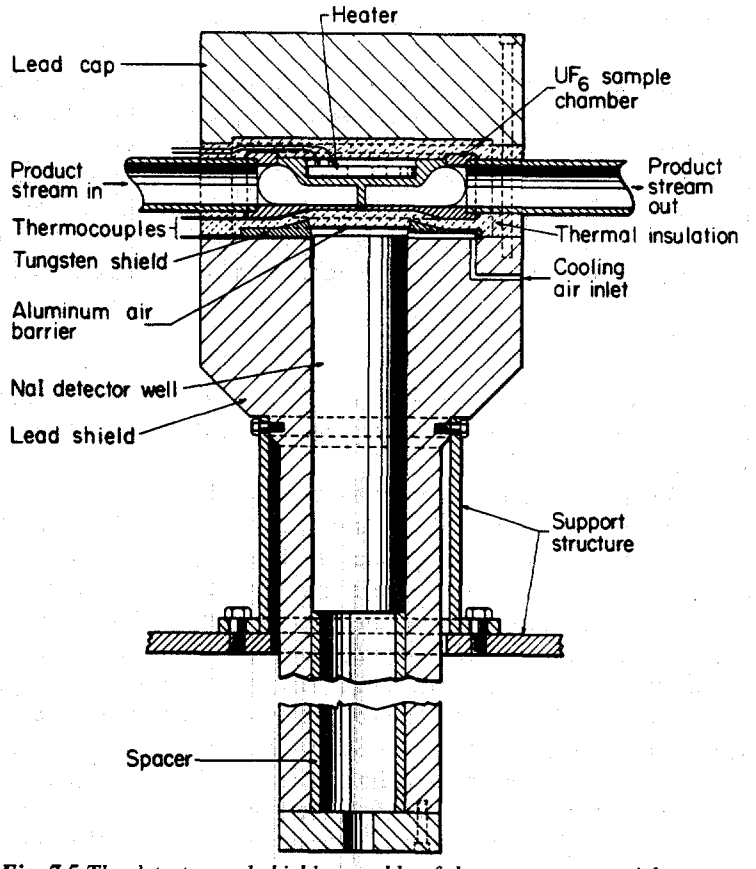

Fig. 7.5 *The detector and shield assembly of the gamma-ray enrichment meter at the Portsmouth GDP. The liquid UF_6 product flows through the sample chamber, where the 186-keV gamma-ray intensity is measured to determine the UF_6 enrichment. (Figure from Ref. 9.)*

While not strictly an infinite-thickness technique, there is a procedure used in the analytical chemistry laboratories of some fuel processors, such as General Electric in Wilmington, North Carolina, that deserves mention. Small samples of process materials are dissolved and prepared as dilute, aqueous samples of uranyl nitrate in standard ampules. The ^{238}U daughters are removed from the solution before measurement. These samples are inserted in NaI well counters and measured against a carefully prepared range of isotopic standards. The technique can provide a very accurate (0.1–0.2%) assay of uranium enrichment. General Electric measures thousands of samples each year using this technique.

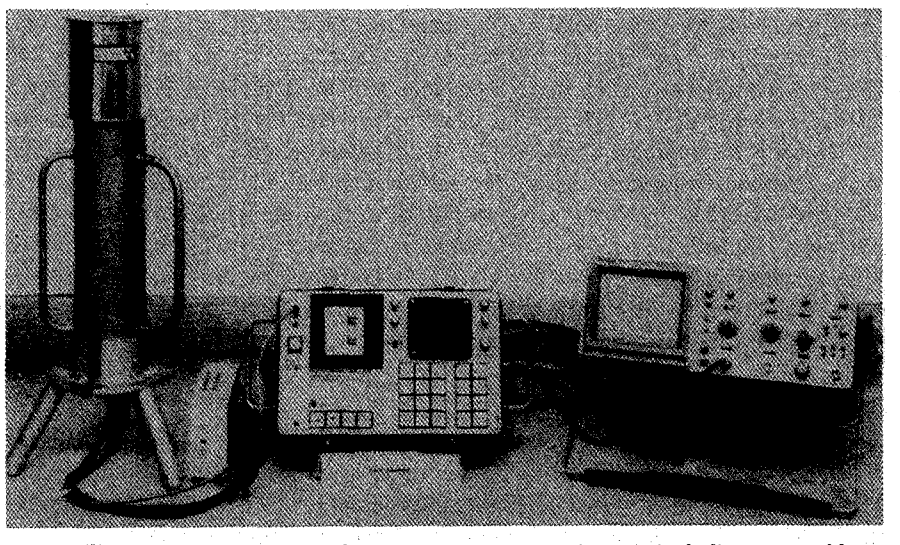

Fig. 7.6 *Gamma-ray uranium enrichment measurement equipment, including a portable, microprocessor-based MCA and a NaI(Tl) gamma-ray detector. This instrumentation can be battery powered and is suited for mobile field applications.*

7.4 PEAK-RATIO TECHNIQUES

7.4.1 Theory

For arbitrary, noninfinite uranium samples (for example, thin foils, contamination deposits, or dilute solutions), it is difficult to correct the 186-keV gamma intensity for absorption in order to yield enrichment. This difficulty arises because the factor $[1 - \exp(-\mu\rho D)]$ in Equation 7-8 is difficult to estimate. The peak-ratio technique requires the measurement of *ratios* of gamma-ray intensities from the major isotopes and the use of that information to determine the uranium enrichment. The technique is basically identical to the plutonium isotopic analysis procedure described in Chapter 8. In the simplest case of low ^{235}U enrichment, ^{235}U and ^{238}U are essentially the only components. Since the sum of their isotopic fractions (f) is then equal to 1, the ^{235}U atom enrichment is (recall Equation 7-2)

$$E_a = f_{235} = N(235)/[N(235) + N(238)] = (1 + f_{238}/f_{235})^{-1} . \qquad (7\text{-}13)$$

If ^{234}U or ^{236}U is present in the sample in significant amounts, one can measure other gamma peak ratios that involve these isotopes. Then the expression for the ^{235}U atom enrichment will contain these other ratios. (For an example relating to plutonium isotopic analysis, see Chapter 8.)

The main challenge to the peak-ratio technique is the determination of the isotopic ratio f_{238}/f_{235}. The most intense gamma-ray peaks from ^{238}U are those in the 700- to 1000-keV energy range from its ^{234m}Pa daughter (see Table 7-1). The large energy difference between the ^{234m}Pa (^{238}U) gamma rays and the 186-keV ^{235}U gamma ray necessitates a significant correction for the different relative detection efficiencies (including photon absorption through the sample material and container). Establishing this relative efficiency curve as a function of energy requires the measurement of known peak intensities over the energy range of interest. (See Chapter 8 for details relating to plutonium isotopic analysis.) For uranium measurements, one must determine several gamma intensities from the two main isotopes (^{235}U and ^{238}U) and normalize the measurements to a common efficiency curve.

7.4.2 Applications

In one application of this procedure, the normalization factor k between the relative efficiency curves for the ^{235}U gamma intensities and the ^{238}U intensities is determined iteratively (Ref. 12). The atom enrichment in Equation 7-13 then becomes

$$E_a = [1 + k\,(\lambda_{235}/\lambda_{238})]^{-1} \tag{7-14}$$

where λ_A is the nuclear decay constant for the uranium isotope of mass A, and k is the iteratively determined ratio of the two activities of the isotopes of interest:

$$k = A(^{238}U)/A(^{235}U)\ . \tag{7-15}$$

To determine the relative efficiency curve, a weak ^{234m}Pa gamma ray at 258.3 keV and a ^{234}Th gamma ray at 63.3 keV are included to extend the efficiency data from ^{238}U decay to the energy region where ^{235}U gamma rays are prominent.

A similar philosophy has been applied (Refs. 13 through 16) with the use of high-resolution gamma-ray spectroscopy in the narrow 89- to 99-keV energy range. In one approach (Refs. 13 through 15) the lines used for isotopic measurements were situated in the 92.4- to 93.4-keV range: the intensities of the 92.4- and 92.8-keV lines of ^{234}Th were used as a measure of the ^{238}U concentration of the sample, and the 93.35-keV thorium $K_{\alpha 1}$ line was used as a measure of the ^{235}U concentration. The ^{238}U contribution to the 93.35-keV line was taken into account in the calibration. Uranium K_α x rays were used for the energy and efficiency calibrations. Better than 1% agreement with mass-spectroscopic analyses was achieved in laboratory studies. Another approach (Ref. 16) used the 89.9-keV thorium K x ray from ^{235}U decay and the 92-keV gamma-ray doublet from ^{234}Th; the results agreed with standard values to within 1%.

Both of the low-energy peak-area ratio techniques rely on the equilibrium between the ^{234}Th daughter and the ^{238}U parent. Since the half-life of ^{234}Th is 24 days, equilibrium is usually achieved in 120 to 168 days (97% and 99%, respectively, of

equilibrium activity) after chemical separation. The narrow energy range minimizes uncertainties in the energy-dependent relative photopeak efficiencies, and the empirical determination of these efficiencies for each sample makes this enrichment measurement technique less dependent on knowledge of the matrix materials. However, neither of the low-energy techniques has yet found significant field application.

7.4.3 Summary of Peak-Ratio Techniques

The methods described above have the advantage that peak *ratios* are measured, allowing the uranium enrichment to be determined without the use of enrichment standards or the determination of geometry-dependent calibration constants. In addition, the samples do not need to satisfy the infinite-thickness criterion. Furthermore, the relative efficiency corrections are made for each sample and include not only the absorption by the sample material but also that by the sample container and any external absorbers. The plutonium isotopics measurements described in Chapter 8 have the same advantages. The disadvantages of this technique are related to

- The low intensity of the ^{238}U daughter radiation for the higher-energy method
- The need for secular equilibrium between the ^{238}U and its daughters
- The need for isotopic homogeneity in the sample.

The need for isotopic homogeneity manifests itself in cases where residual sample material from other sources may be in the container with the material currently being measured—for example, in the measurement of UF_6 cylinders in which uranium from previous shipments may have deposited on the walls of the cylinder.

The peak ratio methods of determining uranium enrichment can also, in principle, be applied to "infinite" samples. However, in those cases, the peak-ratio methods are more cumbersome and time-consuming and usually have no advantage over the enrichment-meter technique, which is simpler, faster, and less expensive.

7.5 GAS-PHASE URANIUM ENRICHMENT MEASUREMENT TECHNIQUES

An extreme case of performing enrichment measurements on a noninfinite sample is the measurement on UF_6 in the gaseous phase. In one technique (Refs. 17 through 20) the ^{235}U concentration was determined from a measurement of the 186-keV gamma-ray emission rate R from the decay of ^{235}U, and the total uranium concentration was determined by measuring the transmission (T_{60}) through UF_6 gas of 60-keV gamma rays from an external ^{241}Am source. Figure 7.7 shows the measurement system, with the orientation of the NaI(Tl) detector and the sample chamber and the location of the ^{241}Am transmission source. The (atomic) enrichment E_a was related to the measured count rate R of the 186-keV rays by

$$E_a = R/(C \ln T_{60}) \qquad (7\text{-}16)$$

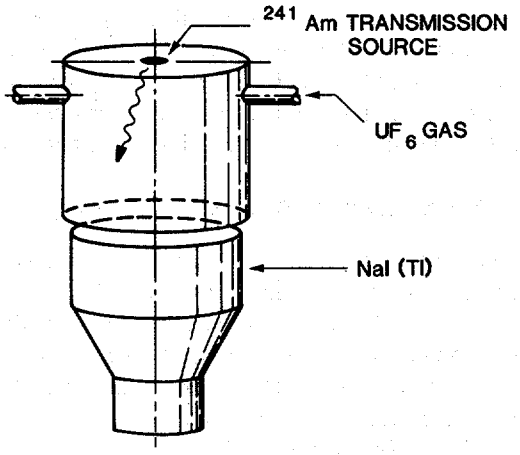

Fig. 7.7 The NaI(Tl)-based gas-phase UF_6 enrichment monitor. The NaI detector views 60-keV gamma rays from the ^{241}Am source (for transmission measurement) and 186-keV gamma rays from the sample chamber (for ^{235}U determination). (Figure from Ref. 18.)

where R was corrected for deadtime losses and attenuation in the gas, C was a calibration constant, and $\ln(T_{60})$ was proportional to the total uranium in the sample. Since the measurement accounted for variations in UF_6 density, the measured assay was independent of the UF_6 pressure. This method produced assay results with measured accuracies better than 1% relative over the range of UF_6 enrichments of 0.72 to 5.4 at%, using a single-point calibration. For 1.0%-enriched UF_6 at 700 torr, a 0.74% relative precision was obtained for a 1000-s counting time (Ref. 19). This technique was applied at relatively high UF_6 pressures; so the data signals were dominated by radiation from the UF_6 gas, making interferences from uranium deposits on the inner surface of the sample chamber unimportant. A NaI(Tl) gamma-ray detector was used during test and evaluation of this instrument in 1982 at the Paducah product feed line of the Oak Ridge Gaseous Diffusion Plant (ORGDP). The instrument was modified for high-resolution gamma-ray detection and tested in 1983. A prototype of the high-resolution instrument (Refs. 20 and 21) for the Portsmouth Gas Centrifuge Enrichment Plant (GCEP) was built and tested at the ORGDP in 1984 (see Figure 7.8).

At lower UF_6 pressures (for example, tens of torr) the density of the UF_6 gas is not great enough for a transmission measurement to have sufficient sensitivity. Furthermore, the radiation from material deposited on the container surfaces becomes a significant fraction of the total signal, and careful corrections for this interference are then required for accurate results. Passive gamma-ray counting and (active) x-ray fluorescence have been combined to verify the approximate enrichment of gaseous UF_6 at low pressures in cascade header pipework (Refs. 22 through 26). The gamma-ray intensities from the decay of ^{235}U (186 keV) and^{238}U daughter products in the pipework deposits and the UF_6 gas were measured to determine the ^{235}U present in

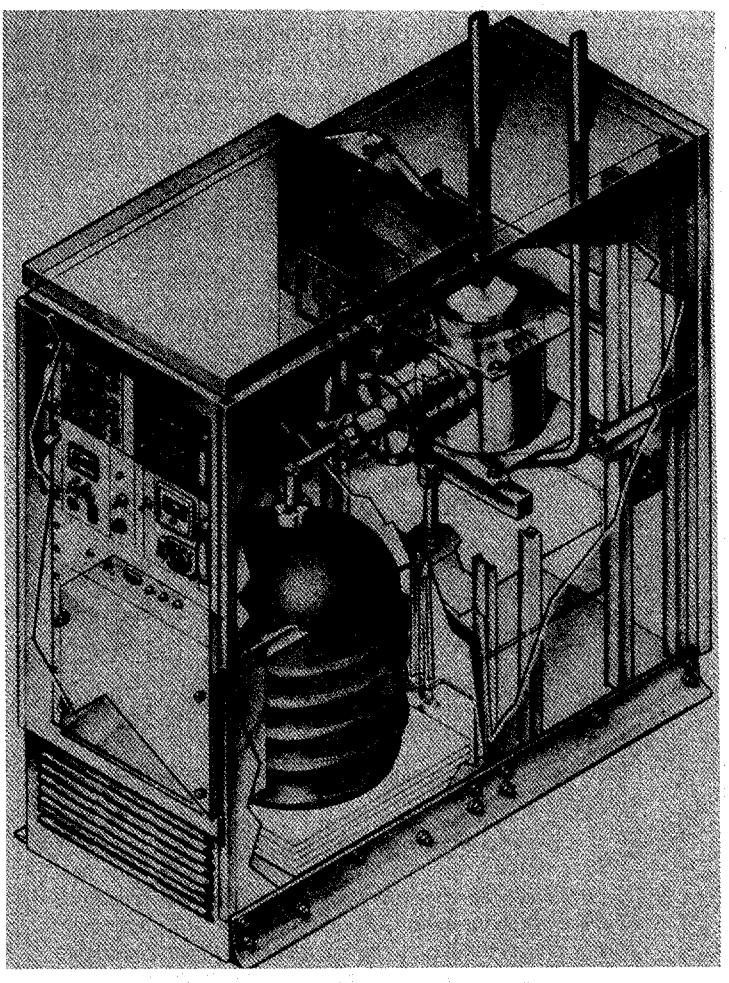

Fig. 7.8 *The UF_6 gas-phase enrichment monitor cabinet for the Portsmouth GCEP. Half of the cabinet houses the detector and electronics, and the other half contains the heated chamber for UF_6 and its associated hardware. (Figure from Ref. 21.)*

the gas. The correction for radiation from the uranium deposited on the inner surface of the pipework was established with gamma rays from ^{234}Th and ^{231}Th decays (Refs. 25 and 26). The total mass of uranium in the gas was measured using x-ray fluorescence with the 122-keV gamma rays from a ^{57}Co excitation source. The ratio of the intensities of the 186-keV gamma rays from the UF_6 gas to the uranium $K_{\alpha 1}$ x rays was calibrated to give a direct measurement of the gas enrichment. A variation

of the correction for uranium deposits (Refs. 24 through 26) determined the correction for the deposited uranium by passive gamma-ray measurements under two different collimation conditions (see Figure 7.9). In both applications, the instruments were capable of providing a "go/no-go" decision on whether the measured enrichment was less than or greater than 20%, thus providing the capability of detection of highly enriched uranium for enrichment plant safeguards.

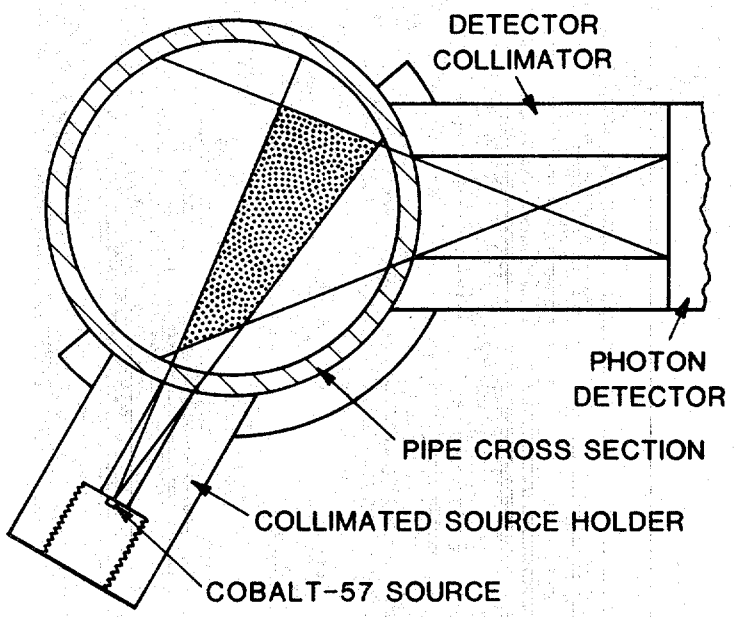

***Fig. 7.9** The detector/collimator arrangement for the enrichment measurement of low-pressure UF_6 in pipe work. The assembly consists of a collimated source holder and detector collimator rigidly connected to the pipework. The overlap of the two fields of view isolates a volume of gas in the middle of the pipe from the wall deposits. A tiny ^{57}Co source is used to fluoresce x rays in the gas. (Figure from Ref. 24.)*

7.6 NEUTRON-BASED ENRICHMENT MEASUREMENTS

Another passive technique for verification of uranium enrichment of UF_6 is the detection of neutrons emitted from the sample as a result of $^{19}F(\alpha,n)$ reactions (Ref. 27). Uranium-234 is the dominant alpha emitter in enriched uranium and hence, indirectly, the principal source of neutrons in UF_6. Also, because the enrichment of ^{234}U follows

the enrichment of ^{235}U, passive total neutron counting can provide a rough measure of ^{235}U enrichment. The ratio of $^{235}U/^{234}U$ may vary by as much as a factor of 4 over the range of depleted to highly enriched uranium for the gaseous diffusion enrichment process; but for low-enriched uranium (<5%), it is more nearly constant, and verification measurements of limited accuracy may be possible without specific ^{234}U isotopic data (Refs. 6, 9, and 28). Further discussion of this technique is presented in Chapter 15.

7.7 CONTAINER WALL ATTENUATION CORRECTIONS

The standard relationship between the enrichment and the measured data (Equation 7-8) includes the term $\exp(\mu_c\rho_c t_c)$ that corrects for the attenuation of the measured radiation by the walls of the sample container. The attenuation may be included in the calibration if the calibration standards and the unknown samples have the same type of container. In some cases this simplification is not possible, and a container wall attenuation correction must be applied in each measurement. This section considers correction methods for an infinite-thickness enrichment measurement where the sample matrix is constant. If T_x, the transmission of one wall thickness of the unknown sample container, is defined by

$$T_x = \exp[-(\mu_c\rho_c t_c)_x] \tag{7-17}$$

and T_s is similarly defined as the container wall transmission in the calibration measurements, then the unknown enrichment is

$$E = KR(E_A)T_s/T_x \tag{7-18}$$

where K is the calibration constant, and $R(E_A)$ is the net gamma-ray peak count rate from the unknown sample at the assay energy (E_A = 186 keV), measured through the container wall. The discussion that follows presents two methods for determining this container attenuation correction, T_s/T_x. In addition, the verification of UF_6 cylinders is discussed to provide an example of a class of measurements where this correction is especially critical.

7.7.1 Direct Measurement of Wall Thickness

If the container composition and wall thickness at the measurement point are known for both the calibration and sample measurements, then T_s/T_x can be calculated directly from the exponential expression

$$T_s/T_x = \exp[(\mu_c\rho_c t_c)_s - (\mu_c\rho_c t_c)_x] \tag{7-19}$$

where ρ_c represents the density of the container material and μ_c is evaluated at the assay energy. The container wall thickness (t_c) can be measured directly using an ultrasonic thickness gauge (See Figure 7.10). A burst of ultrasound is transmitted by

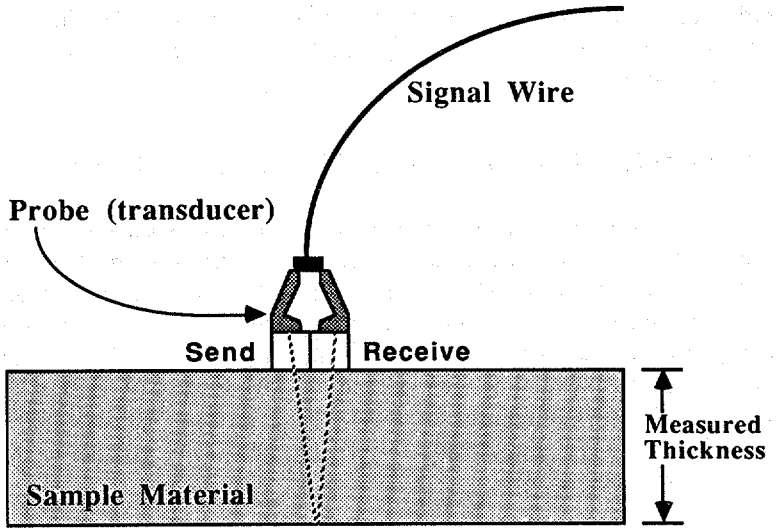

Fig. 7.10 *Probe placement in an ultrasonic measurement of thickness. The probe must be acoustically coupled to the outer surface of the material for the ultrasound pulse to enter the material without being severely attenuated. The coupling is accomplished with a liquid compound (usually supplied with the thickness gauge) placed between the probe face and the material surface.*

the probe into the container material and travels until it reaches a material of substantially different physical character from the container material. The sound is then reflected back to the probe. The gauge electronics performs a precise measurement of the time needed for the ultrasound pulse to make the round trip in the container material and thereby determines the thickness of the material. Such thickness gauges are available commercially, and thickness results can be read usually to ±0.1 mm. Recent calibration measurements (Ref. 29) showed a fluctuation of ±0.055 mm from repeated measurements on a calibrated steel disc having a thickness of 13.500 mm, which corresponds to a relative standard deviation of 0.4%.

7.7.2 Internal-Line Ratio Technique

The transmission ratio T_s/T_x can also be determined from the ratio of intensities of different-energy gamma rays from one isotope, assuming the sample material

is infinitely thick for the gamma rays measured (see Section 7.3.2). Generally, high-resolution gamma-ray spectroscopy is required to resolve the peaks of interest. For corrections to ^{235}U enrichment measurements, there are several reasonably intense gamma rays near the 186-keV peak energy (see Table 7-1). Consider a case in which the intensities of a peak above and a peak below the 186-keV gamma ray (at energies E_H and E_L, respectively) are measured in addition to the assay peak area. With the transmission as defined in Equation 7-17, we have

$$\frac{T_s(E_A)}{T_x(E_A)} = \left[\frac{T_x(E_H)/T_s(E_H)}{T_x(E_L)/T_s(E_L)}\right]^{\frac{\mu_A}{\mu_L-\mu_H}} \tag{7-20}$$

where the subscripts of the μ's refer to the energies at which the μ's are evaluated. To simplify the calculation of the transmission ratios at E_H and E_L, we recall the definition of transmission from the measurement point of view:

$$T = R/R_0 \ . \tag{7-21}$$

Here, R is the measured peak count rate, attenuated by the container wall, and R_0 is the measured peak count rate from a sample with an infinitesimally thin container (that is, $t_c \rightarrow 0$). In practice, R_0 cannot be measured, but since the expression in Equation 7-20 contains transmission *ratios*, we can re-express these ratios in terms of ratios of *measured peak areas*:

$$\frac{T_s(E_A)}{T_x(E_A)} = \left[\frac{R_x(E_H)/R_s(E_H)}{R_x(E_L)/R_s(E_L)}\right]^{\frac{\mu_A}{\mu_L-\mu_H}} \tag{7-22}$$

where $R(E_{H,L})$ is the peak area at energy $E_{H,L}$. The fractional error in the transmission ratio T_s/T_x is just the exponent $\mu_A/(\mu_L - \mu_H)$ times the fractional error of the measured peak-area ratio expression in the bracket on the right of Equation 7-22. Thus, it is advantageous to make the exponent as small as possible, which means selecting peaks that are not too close in energy. Table 7-4 shows values for the exponent for two commonly encountered container materials and two choices of measurement peaks. Note that one choice includes the ^{235}U assay peak.

Although the internal-line ratio technique is a convenient technique for determining the container attenuation correction, there are no published accounts of its application in enrichment measurements. The major difficulty with using the technique is the time required to obtain adequate statistical precision in the auxiliary gamma-ray peak areas.

Table 7-4. Values of exponent function $\mu_A/(\mu_L - \mu_H)$ for common container materials

E_H/E_L	Iron	Monel	Aluminum	Polyethylene[a]
205 keV/144 keV	2.57	2.17	8.13	8.88
186 keV/144 keV	3.20	2.78	11.09	11.83

[a]Low-density polyethylene, as used in containers.

7.7.3 Measurement of UF_6 Cylinders

One of the most common container types in enrichment measurements is the large cylinder used to ship and store UF_6 in liquid or solid form. These cylinders vary in size and wall thickness. Table 7-5 gives some pertinent parameters for the most common cylinder types (Ref. 30). The large, high-density wall thicknesses of the cylinders means that minor variation in wall thickness can result in significant variation in gamma-ray count rate. The relationship between the relative fluctuation of the enrichment result and the relative fluctuation of the wall thickness is obtained by differentiation of Equation 7-8:

$$dE/E = \mu_c \rho_c (dt_c/t_c) = 1.12(dt_c/t_c) \tag{7-23}$$

where the second result is for steel ($\mu_c = 0.144$ cm^2/g at 186 keV and $\rho_c = 7.8$ g/cm^3). Thus, a 10% variation in cylinder wall thickness (only 0.05 in. for type 30B cylinders) will cause a 12% bias in the corresponding enrichment measurement. Use of a thickness-gauge measurement of the wall thickness reduces the measurement error to a few tenths of one percent, essentially removing the wall thickness from consideration as a source of measurement bias. The UF_6 enrichment measurement apparatus for cylinders can be calibrated by using one or more cylinders as standards, which may then be sampled for analysis. Alternatively, standards of U_3O_8 or UF_4 of known enrichment may be used, with the appropriate corrections for matrix differences (that is, the factor F/F_s in Table 7-3).

Early studies of enrichment measurements on type 30B and 5A cylinders with NaI scintillation detectors (Ref. 6) achieved assay results with relative standard deviations of 5% for type 30B cylinders and <1% for type 5A cylinders. Count times were on the order of a few minutes, and the wall thickness measurement took only a few seconds. Good acoustic coupling between the thickness-gauge probe and the cylinder surface was obtained by sanding the paint off a spot within the area viewed by the gamma-ray detector; the uncertainty in the thickness measurement was estimated at 0.4%. A more recent study of enrichment measurements on type 48 and 30 UF_6 cylinders (Ref. 28) achieved similar results, even with the use of high-resolution gamma-ray detection equipment.

Table 7-5. Physical characteristics of selected UF_6 storage and shipping cylinders[a]

	Cylinder Type			
Characteristic	5A	8A	30B	48X
Nominal diameter (in.)	5	8	30	48
Nominal length (in.)	36	56	81	121
Material of construction	Monel	Monel	steel	steel
Wall thickness (in.)	1/4	3/16	1/2	5/8

[a]Ref. 30.

7.8 EXTENSION OF THE ENRICHMENT METER PRINCIPLE TO OTHER APPLICATIONS

7.8.1 Concentration Meter

Under certain limits of uranium concentration, uranium measurements using the enrichment meter principle become uranium *concentration* measurements (Ref. 5). The same mathematical expressions govern both cases (Equation 7-8); the dependence of the result on the uranium and matrix concentrations is contained in the factor F in Equation 7-9. For matrices with effective $Z \leq 30$, the ratio μ_m/μ_U is less than 0.1. Then for $\rho_m/\rho_U \leq 1$, the value of the correction factor F is very close to 1, and the count rate is almost directly proportional to the enrichment:

$$R = KEF = KE \, . \tag{7-24}$$

The domain in which $\mu_m\rho_m/\mu_U\rho_U \leq 0.1$ is therefore referred to as the "enrichment domain."

At the other end of the spectrum are measurements for which the uranium concentration is very low compared with that of the matrix. In cases where $\mu_m\rho_m/\mu_U\rho_U \geq 10$, the unity term in F can be ignored. Then, if the enrichment and μ values are known, Equation 7-24 becomes

$$R = KEF = K'E(\rho_U/\rho_m) \tag{7-25}$$

with an error of $\leq$10%. K′ is another calibration constant. The domain for which $\mu_m\rho_m/\mu_U\rho_U \geq 10$ can therefore be called the "concentration meter" domain. The infinite-thickness criterion still must be met in this domain. Examples of samples that would fall into the concentration domain are containers with uranium-contaminated material such as dilute uranium-bearing solutions or uranium holdup in a Raschig-ring tank (Ref. 5).

7.8.2 Mixing (Blend) Ratio in Mixed-Oxide Fuel

The enrichment meter concept may also be used for quality control of different reactor-fuel blends, for example, PuO_2, UO_2, U-C, and Th-C, or in general for the assay of any fissionable material having a suitable low-energy gamma ray so that the sample satisfies the infinite-thickness criterion (Refs. 4 and 31). In the more general case of mixtures of several components, the counting rate from a specific gamma ray from an isotope with enrichment E is given by

$$R = ESA\varepsilon/(\mu_1 F) \tag{7-26}$$

where F is now the more general form of the expression in Equation 7-9:

$$F = 1 + \left[1/(\mu_1\rho_1)\right] \sum_{i=2}^{n} \mu_i\rho_i \ . \tag{7-27}$$

The running index i denotes the relevant elemental constituents in the blend of materials in the sample, and the specific subscript 1 denotes the element whose isotope emits the "signal" gamma ray of interest. For the case of a PuO_2 + UO_2 blend and the detection of a plutonium ("signal") gamma ray (the 129-keV gamma ray meets the infinite-thickness criterion), the above expression reduces to

$$R = \frac{ESA\varepsilon}{\mu_{Pu}K(1+r)} \tag{7-28}$$

where r is the blending ratio, ρ_U/ρ_{Pu}. The constant K reflects the higher-order contributions from the matrix and the SNM mixture and has values near unity. The fraction 1/(1+r) reflects the essential change in attenuation of plutonium gamma rays by the addition of uranium. Since K is quite insensitive to gross changes in the blending ratio (Ref. 4), the response of an infinite-sample enrichment measurement is therefore directly proportional to E/(1+r); that is, it will sense variations in either the isotopic enrichment or the blending ratio. Concurrent measurement of one of the uranium gamma rays in this example could, in principle, permit monitoring of both the plutonium enrichment and the blending ratio independently, provided the uranium isotopic composition were known.

REFERENCES

1. M. E. Anderson and J. F. Lemming, "Selected Measurement Data for Plutonium and Uranium," Mound Laboratory report MLM-3009 (1982).

2. T. R. Canada, *An Introduction to Non-Destructive Assay Instrumentation, A Training Manual for the International Atomic Energy Agency Inspectorate*, (International Atomic Energy Agency, Vienna, 1984).

3. J. T. Russell, "Method and Apparatus for Nondestructive Determination of ^{235}U in Uranium," US Patent No. 3 389 254, June 1968.

4. T. D. Reilly, R. B. Walton, and J. L. Parker, "The Enrichment Meter—A Simple Method for Measuring Isotopic Enrichment," in "Nuclear Safeguards Research and Development Program Status Report, September–December, 1970," G. Robert Keepin, Comp., Los Alamos Scientific Laboratory report LA-4605-MS (1970), p. 19.

5. J. L. Parker and T. D. Reilly, "The Enrichment Meter as a Concentration Meter," in "Nuclear Analysis Research and Development, Program Status Report, September–December 1972," G. Robert Keepin, Comp., Los Alamos Scientific Laboratory report LA-5197-PR (1972), p. 11.

6. R. B. Walton, T. D. Reilly, J. L. Parker, J. H. Menzel, E. D. Marshall, and L. W. Fields, "Measurement of UF_6 Cylinders with Portable Instruments," *Nuclear Technology* 21, 133 (1974).

7. L. A. Kull and R. O. Ginaven, "Guidelines for Gamma-Ray Spectroscopy Measurements of ^{235}U Enrichment," Brookhaven National Laboratory report BNL-50414 (1974).

8. P. Matussek, "Accurate Determination of the ^{235}U Isotope Abundance by Gamma Spectrometry: A User's Manual for the Certified Reference Material EC-NRM-171/NBS-SRM-969," Institut für Kernphysik report KfK 3752, Kernforschungszentrum, Karlsruhe, Federal Republic of Germany (1985).

9. T. D. Reilly, E. R. Martin, J. L. Parker, L. G. Speir, and R. B. Walton, "A Continuous In-Line Monitor for UF_6 Enrichment," *Nuclear Technology* 23, 318 (1974).

10. J. K. Halbig, S. F. Klosterbuer, and R. A. Cameron, "Applications of a Portable Multichannel Analyzer in Nuclear Safeguards," Proc. of the IEEE 1985 Nuclear Science Symposium, San Francisco, California, October 23-25, 1985. Also available as Los Alamos National Laboratory document LA-UR-85-3735 (1985).

11. D. R. Terry, "Development of IAEA Safeguards Measurements for Enrichment Plants," *Transactions of the American Nuclear Society* 50, 176 (1985).

12. R. J. S. Harry, J. K. Aaldijk, and J. P. Braak, "Gamma-Spectroscopic Determination of Isotopic Composition Without Use of Standards," *Proc. IAEA Symposium, "Safeguarding Nuclear Materials,"* Vienna, October 20-24, 1975, Vol. II (1975), p. 235.

13. T. N. Dragnev and B. P. Damyanov, "Methods for Precise, Absolute Gamma-Spectrometric Measurements of Uranium and Plutonium Isotopic Ratios," *Proc. IAEA Symposium on Nuclear Material Safeguards*, Vienna, Austria, October 2-6, 1978, IAEA-SM-231, Vol. I (1978), p. 739.

14. T. N. Dragnev, B. P. Damyanov, and K. S. Karamanova, "Non-Destructive Measurements of Uranium and Thorium Concentrations and Quantities," *Proc. of the IAEA Symposium on Nuclear Material Safeguards*, Vienna, Austria, October 2-6, 1978, IAEA-SM-231, Vol. II (1978), p. 207.

15. T. N. Dragnev, B. P. Damyanov, and G. G. Grozev, "Simplified Procedures and Programs for Determining Uranium and Plutonium Isotopic Ratios," *Proc. IAEA Symposium on Nuclear Material Safeguards*, Vienna, Austria, November 8-12, 1982, IAEA-SM-260, Vol. II (1982), p. 258.

16. R. Hagenauer, "Nondestructive Determination of Uranium Enrichment Using Low-Energy X and Gamma Rays," *Nuclear Materials Management* XI, 216 (1982).

17. J. W. Tape, M. P. Baker, R. Strittmatter, M. Jain, and M. L. Evans, "Selected Nondestructive Assay Instruments for an International Safeguards System at Uranium Enrichment Plants," *Nuclear Materials Management* VIII, 719 (1979).

18. R. B. Strittmatter, J. N. Leavitt, and R. W. Slice, "Conceptual Design for the Field Test and Evaluation of the Gas-Phase UF_6 Enrichment Meter," Los Alamos Scientific Laboratory report LA-8657-MS (1980).

19. R. B. Strittmatter, "A Gas-Phase UF_6 Enrichment Monitor," *Nuclear Technology* 59, 355 (1982).

20. R. B. Strittmatter, L. A. Stovall, and J. K. Sprinkle, Jr., "Development of an Enrichment Monitor for the Portsmouth GCEP," *Proc. Conference on "Safeguards Technology: The Process-Safeguards Interface,"* Hilton Head Island, SC, November 28-December 3, 1983, (Conf. 831106, 1984), p. 63.

21. R. B. Strittmatter, R. R. Pickard, J. K. Sprinkle, Jr., and J. R. Tarrant, "Data Evaluation of a Gas-Phase UF_6 Enrichment Monitor," *Proc. ESARDA/INMM Joint Specialist Meeting on NDA Statistical Problems*, Ispra, Italy, September 12-14, 1984, p. 243.

22. D. A. Close, J. C. Pratt, H. F. Atwater, J. J. Malanify, K. V. Nixon, and L. G. Speir, "The Measurement of Uranium Enrichment for Gaseous Uranium at

Low Pressure," *Proc. of the 7th Annual Symposium on Safeguards and Nuclear Material Management, ESARDA*, Liege, Belgium, May 21-23, 1985, p. 127.

23. D. A. Close, J. C. Pratt, J. J. Malanify, and H. F. Atwater, "X-Ray Fluorescent Determination of Uranium in the Gaseous Phase," *Nuclear Instruments and Methods A* 234, 556 (1985).

24. D. A. Close, J. C. Pratt, and H. F. Atwater, "Development of an Enrichment Measurement Technique and its Application to Enrichment Verification of Gaseous UF_6," *Nuclear Instruments and Methods A* 240, 398 (1985).

25. T. W. Packer and E. W. Lees, "Measurement of the Enrichment of Uranium in the Pipework of a Gas Centrifuge Plant," *Proc. 6th Annual Symposium on Safeguards and Nuclear Material Management, ESARDA*, Venice, Italy, May 14-18, 1984, p. 243.

26. T. W. Packer and E. W. Lees, "Measurement of the Enrichment of UF_6 Gas in the Pipework of a Gas Centrifuge Plant," *Proc. 7th Annual Symposium on Safeguards and Nuclear Material Management, ESARDA*, Liege, Belgium, May 21-23, 1985, p. 299.

27. T. D. Reilly, J. L. Parker, A. L. Evans, and R. B. Walton, "Uranium Enrichment Measurements on UF_6 Product Cylinders," in "Nuclear Safeguards Research and Development, Progress Status Report, May–August 1971," G. Robert Keepin, Comp., Los Alamos Scientific Laboratory report LA-4794-MS (1971), p. 16.

28. J. L. Weiman, "Practical Uncertainty Limits in Gamma-Ray Enrichment Measurements on Low-Enriched Uranium Hexafluoride," *Proc. ESARDA/INMM Joint Specialist Meeting on NDA Statistical Problems*, Ispra, Italy, September 12-14, 1984, p. 101.

29. L. R. Stieff, R. B. Walton, T. D. Reilly, L. W. Fields, R. L. Walker, W. T. Mullins, and J. I. Thoms, "Neutron Measurements of ^{234}U Isotopic Abundances in UF_6 Samples," *Nuclear Materials Management* IV, 179 (1975).

30. "Uranium Hexafluoride: Handling Procedures and Container Criteria," Oak Ridge Operations Office report ORO-651, Revision 4 (1977).

31. G. W. Nelson, S. -T. Hsue, T. E. Sampson, and R. G. Gutmacher, "Measurement of Uranium/Plutonium Blending Ratio," in "Safeguards and Security Progress Report, January–December 1984," Darryl B. Smith, Comp., Los Alamos National Laboratory report LA-10529-PR (1986), p. 19.